JOC The Journal of Organic Chemistry

Article

pubs.acs.org/joc

Design of Redox/Radical Sensing Molecules via Nitrile Imine-Mediated Tetrazole-ene Cycloaddition (NITEC)

Paul Lederhose,[†,‡,#] Naomi L. Haworth,[§] Komba Thomas,[†] Steven E. Bottle,[†] Michelle L. Coote,[§] Christopher Barner-Kowollik,*[,†,‡,#] and James P. Blinco*[,†]

[†]School of Chemistry, Physics and Mechanical Engineering, Faculty of Science and Technology, Queensland University of Technology, Queensland 4001, Australia

[‡]Preparative Macromolecular Chemistry, Institut für Technische Chemie und Polymerchemie, Karlsruhe Institute of Technology (KIT), Engesserstr. 18, 76131 Karlsruhe, Germany

[#]Institut für Biologische Grenzflächen, Karlsruhe Institute of Technology (KIT), Hermann-von-Helmholtz-Platz 1, 76344 Eggenstein-Leopoldshafen, Germany

[§]ARC Centre of Excellence for Electromaterials Science, Research School of Chemistry, The Australian National University, Canberra, ACT 2601, Australia

Supporting Information

ABSTRACT: The current study introduces a novel synthetic avenue for the preparation of profluorescent nitroxides via nitrile imine-mediated tetrazole-ene cycloaddition (NITEC). The photoinduced cycloaddition was performed under metal-free, mild conditions allowing the preparation of a library of the nitroxide functionalized pyrazolines and corresponding methoxyamines. High reaction rates and full conversion were observed, with the presence of the nitroxide having no significant impact on the cycloaddition performance. The formed products were investigated with respect to their photophysical properties in order to quantify their "switch on/off" behavior. The fluorescence quenching performance is strongly dependent on the distance between the chromophore and the free radical spin as demonstrated theoretically and experimentally. Highest levels of fluorescence quenching were achieved for pyrazolines with the nitroxide directly fused to the chromophore. Importantly, the pyrazoline profluorescent nitroxides were shown to efficiently act as sensors for redox/radical processes.

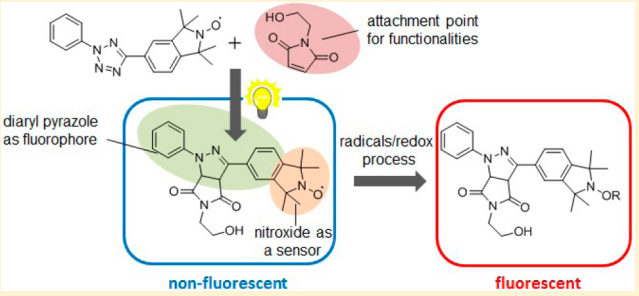

INTRODUCTION

Profluorescent nitroxides (PFNs) are hybrid molecules in which a stable free radical moiety is covalently tethered to a fluorophore. Nitroxides are well-known for their ability to quench the excited states of chromophores (both intramolecularly, when covalently linked to the nitroxide, and intermolecularly, when the nitroxide is in the immediate vicinity of the excited chromophore).[1] The mechanism by which the quenching occurs relies on the paramagnetic nature of the nitroxides. When a fluorophore has been excited from the ground state (S_0) to an excited state (S_n), it will move to the lowest energy excited state (S_1) by energy loss through internal conversion. When a nitroxide radical is present, it facilitates intersystem crossing of excited state electrons of the fluorophore from the excited singlet state to a lower energy triplet state. Return to the singlet ground state from the triplet becomes spin forbidden, and the triplet state of fluorophores linked to the nitroxide is longer lived, and nonradiative release of energy to the surrounding environment is the dominant pathway.[1] Consequently, while the absorbance of the fluorophore remains unchanged, the presence of the nitroxide radical quenches the fluorescence substantially. However, if the nitroxide radical scavenges another radical species or undergoes a one electron redox reaction, the resulting molecule is diamagnetic, the enhanced intersystem crossing ceases, and no quenching of the fluorescence is observed.[2] Using this "on–off" fluorescence, PFNs have found applications as controlling agents for free radical polymerizations[3] and as radical/redox sensors in fields of material science[4−6] and biology[7] where they are widely used in bioimaging.[8−11]

The synthesis of a variety of profluorescent nitroxides has been previously reported through simple linkage of nitroxides and fluorophore via esterification,[2,3,12,13] amidation,[4,5] or sulfonamidation.[7,14,15] These linkages, however, can be sensitive to hydrolysis which, if it occurs, will negate the fluorescence quenching process enabled by the nitroxide. Linkage via carbon–carbon bond formation is a preferred alternative as it provides a much more stable connection.[16−20] Recently, the click chemistry concept[21] was applied to the synthesis of PFNs.

Received: May 15, 2015
Published: July 13, 2015

DOI: 10.1021/acs.joc.5b01088
J. Org. Chem. 2015, 80, 8009−8017

In this approach, an alkyne functionalized isoindoline nitroxide was coupled with an azide-containing fluorophore via copper mediated 1,3-dipolar cycloaddition, with the isoindoline either in the form of a small molecule[22] or attached to a polymeric backbone.[22,23] Copper was required as a catalytic species for this methodology, which limits *in vivo* and healthcare-related applications.[24]

An alternative click process to the CuAAC cycloaddition is the nitrile imine-mediated tetrazole-ene cycloaddition (NITEC), which has recently gained attention in a number of fields of research. This photoinduced, two-step reaction was first reported by Huisgen et al.[25] and has most recently been applied to the modification of proteins[26] and functionalization of surfaces.[27] Advantages of this cyclization include that it proceeds without the need of a (metal) catalyst and that the cycloadduct formation is irreversible. The reaction also achieves high reaction rates and full conversion to the targeted products.[28] Moreover, spatially resolved cycloaddition has been achieved when irradiating well-defined tetrazole-modified surfaces in the presence of an olefin-containing solution, allowing the fabrication of patterned substrates.[27,29−31]

The NITEC involves two steps (Scheme 1).[28] When irradiated with UV light, a nitrile imine is formed via a first-order reaction with the release of nitrogen. The *in situ* generated nitrile imine subsequently undergoes a rapid cycloaddition with the olefin. The resultant pyrazoline displays strong fluorescence due to the formation of a new conjugated system. The photophysical properties of the products are influenced by the nature of the substituents on each of the aryl rings.

Scheme 1. Photo-Triggered 1,3-Dipolar Cycloaddition Between a 2,5-Diaryl Tetrazole and a Substituted Alkene Dipolarophile[28]

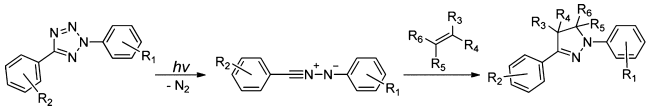

In the current work, we introduce a novel synthetic route to form profluorescent nitroxides using NITEC click chemistry. The method allows for the fast and efficient formation of redox-/radical-sensitive molecules without the need for a metal catalyst (Figure 1). An investigation of the distance and orientation of the linkage between the nitroxide and chromophore was undertaken, and the photophysical properties of several of these compounds were compared. Finally, model reduction and radical scavenging studies were carried out to demonstrate the ability of these newly formed compounds to function as fluorescent sensors.

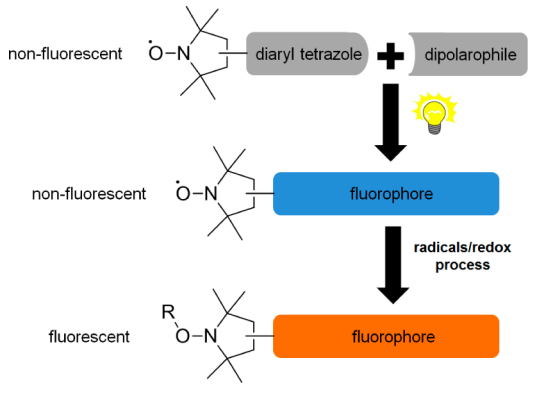

Figure 1. NITEC approach for formation of profluorescent nitroxides.

RESULTS AND DISCUSSION

The choice of reagents for the synthesis of pyrazoline fluorophore linked nitroxides was driven by two major factors. First to be considered is the distance between the diaryl tetrazole and the nitroxide moiety. The mechanism for formation of the nitrile imine includes species from a number of photoexcited states. As nitroxides are well-known quenchers of such excited states it was thought that the presence of the nitroxide in too close proximity to the tetrazole may impact substantially on the efficiency of the nitrile imine formation. The second consideration is the distance between the final pyrazoline fluorophore and the nitroxide. This distance has been shown to be a key factor in the degree of fluorescence quenching observed in the PFN molecule. Shorter distance between the moieties results in more efficient fluorescence quenching. Therefore, the position of the nitroxide with respect to the initial diaryl tetrazole and the final fluorescent pyrazoline need to be carefully considered.

The first generation of pyrazoline PFNs studied was synthesized via a NITEC reaction between the diaryl tetrazole **1** and the nitroxide functionalized maleimide **2**. By avoiding the direct covalent linkage of diaryl tetrazole and the nitroxide, intramolecular quenching effects of the nitroxide on the excited state of the diaryl tetrazole were expected to be limited. The reagents were irradiated in a 1:1 ratio in ACN/DMSO at 254 nm (emission maximum) for 15 min. After this time, both diaryl tetrazole **1** and maleimide **2** were completely consumed, and only the formation of desired free radical-containing pyrazoline **3** was observed (Scheme 2). The structure and purity of compound **3** were demonstrated by high-resolution mass spectrometry (HRMS) and high-performance liquid chromatography (HPLC). The presence of the nitroxide spin in the product was confirmed by the expected three-line electron paramagnetic resonance (EPR) spectrum (see Supporting Information(SI)). As nitroxides are paramagnetic, the NMR of these molecules is generally broad and featureless. Thus, in order to characterize the cycloadduct via NMR, species **3** was converted to the methoxyamine derivative **4** using Fenton chemistry[32] (Scheme 2).

Scheme 2. NITEC of Diaryl Tetrazole 1 and Maleimide 2 To Form Nitroxide Pyrazoline 3[a]

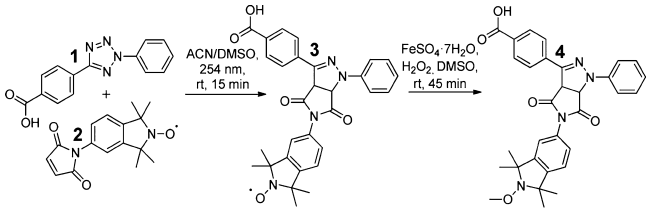

[a]Conversion of formed radical pyrazoline **3** to methoxyamine derivative **4**.

Synthesis of the derivative **4** also gives the opportunity to compare the photophysical properties of the paramagnetic, nitroxide-containing pyrazoline **3** with a diamagnetic analogue, which is a model of the outcome of the PFN radical-scavenging process. To quantify the profluorescent nature of the

DOI: 10.1021/acs.joc.5b01088
J. Org. Chem. 2015, 80, 8009−8017

synthesized compounds, fluorescence measurements on compound **3** and subsequently the diamagnetic derivative **4** were performed. To ascertain the correct wavelength and equivalent concentrations of solutions of radical species and the methoxyamine derivative, optical matching via UV−vis absorbance spectroscopy was employed. A comparison of the fluorescence spectra of **3** with **4** demonstrates the quenching effect when the nitroxide radical species is present (Figure 3). The peak intensity of **3** is approximately 30% less than the peak intensity of the corresponding methoxyamine **4**. While still substantial, the quenching observed for compound **3** is much less than has been observed previously for other PFN molecules synthesized.[1] This is most likely due to a combination of the relatively long distance and poor orientation between the single electron from the nitroxide and the fluorescent pyrazoline moiety of the molecule. This is seen in Figure 2, which shows the optimized geometry of **3**. Not only is

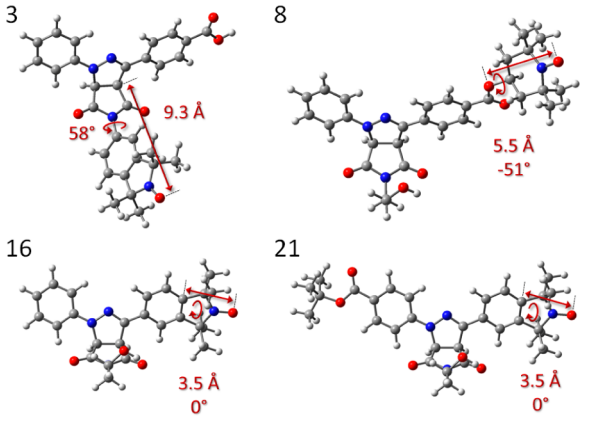

Figure 2. Optimized structures of compounds **3**, **8**, **16**, and **21** showing the distance of the fluorophore from the formal radical center and its distortion from planarity, measured as the dihedral angle between the plane of the fluorophore and a plane perpendicular to the 2p orbital of the nitroxide.

the fluorophore 9.3 Å from the radical center but also the fluorophore is tilted at 58° with respect to the 2p orbital of the radical. Thus, overlap between radical and π system of the fluorophore is expected to be poor.

In order to increase the interaction between fluorophore and nitroxide, and thus generate a higher quenching efficiency, a second-generation pyrazoline PFN was synthesized where the spin system is linked to the aryl ring of the tetrazole. To do this, the hydroxy functionalized TEMPO **5** and diaryl tetrazole **1** were esterified via DCC coupling to form the nitroxide-containing diaryl tetrazole **6** (see Scheme 3). In this case, a direct covalent linkage between tetrazole and the nitroxide is used. Therefore, a decrease in the efficiency of the UV-induced formation of the dipolar intermediate potentially could be induced. Interestingly, the NITEC reaction of nitroxide functionalized tetrazole **6** and hydroxy *N*-maleimide **7** still yielded full conversion of **6** and formation of the desired target molecule **8** under the same mild conditions employed for the first-generation approach (Scheme 3). The structure and purity of compound **8** were demonstrated by HRMS, HPLC, and EPR. Species **8** was also converted to the methoxyamine derivative **9** using Fenton chemistry (Scheme 3).

Fluorescence spectra of compounds **8** and **9** were compared (Figure 3). A much stronger fluorescence quenching effect (ca.

Scheme 3. Esterification of Diaryl Tetrazole 1 and Hydroxy Functionalized Nitroxide 5 To Obtain Radical Diaryl Tetrazole 6[a]

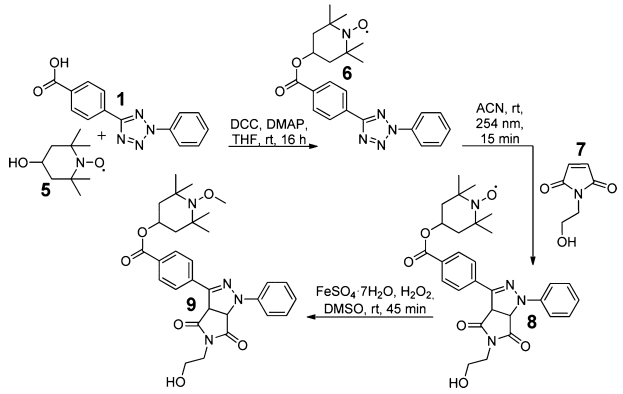

[a]NITEC of radical diaryl tetrazole **6** and maleimide **7** to form radical pyrazoline **8**. Conversion of the radical pyrazoline **8** to methoxyamine **9**.

3-fold compared with the diamagnetic species) was observed for species **8**. The improved quenching performance for the second generation of pyrazolines is due to the shorter distance between the spin and the fluorescent pyrazoline (5.5 Å versus 9.3 Å, see Figure 2). Furthermore, conjugative interaction between the single electron and the pyrazoline through the ester moiety also can potentially enhance the quenching in a through-bond mechanism.

While improved, the level of quenching was still below that of other PFN sensors currently being employed (i.e., 3-fold quenching compared with the literature state-of-art of 300-fold quenching). Moreover, using esterification to attach the nitroxide to the pyrazoline negates much of the benefit of being able to use the NITEC click chemistry for the synthesis of these compounds and leaves the pyrazoline PFNs susceptible to hydrolysis. As there was little impact on the efficacy of the nitrile imine formation, when the nitroxide was covalently linked to the tetrazole moiety, a carbon−carbon linkage between the diaryl tetrazole and the nitroxide moiety was contemplated. Thus, in the third generation of pyrazolines studied, a highly proximate, direct carbon−carbon linkage was envisaged to enhance the PFN "switch on/off" performance. Furthermore, a carbon−carbon linkage should give a much more hydrolytically stable molecule which is of importance if the compounds are to be used as biological sensors. Reaction of the methoxy protected formyl 1,1,3,3-tetramethylisoindoline-2-oxyl **10** and benzenesulfonohydrazide gave intermediate **11**, which was subsequently reacted with diazonium salt **12** to afford the model methoxyamine **13** which could be readily deprotected using *m*CPBA to form the target radical species **14** (Scheme 4). The direct synthesis of the radical species **14** starting from the aldehyde nitroxide was not possible due to complications arising from the reduction of the nitroxide moiety to the hydroxylamine by benzenesulfonohydrazide. The structure and purity of compound **14** were demonstrated by HRMS, HPLC and EPR.

Compounds **13** and **14** were converted in the presence of hydroxy functionalized maleimide **7**—using NITEC—to the pyrazoline derivatives **15** and **16**, respectively (Scheme 5). Again, full conversion of reagents under mild conditions was achieved, even for the free radical-containing pyrazoline **16**. The efficient formation of pyrazoline **15** was expected since

DOI: 10.1021/acs.joc.5b01088
J. Org. Chem. 2015, 80, 8009−8017

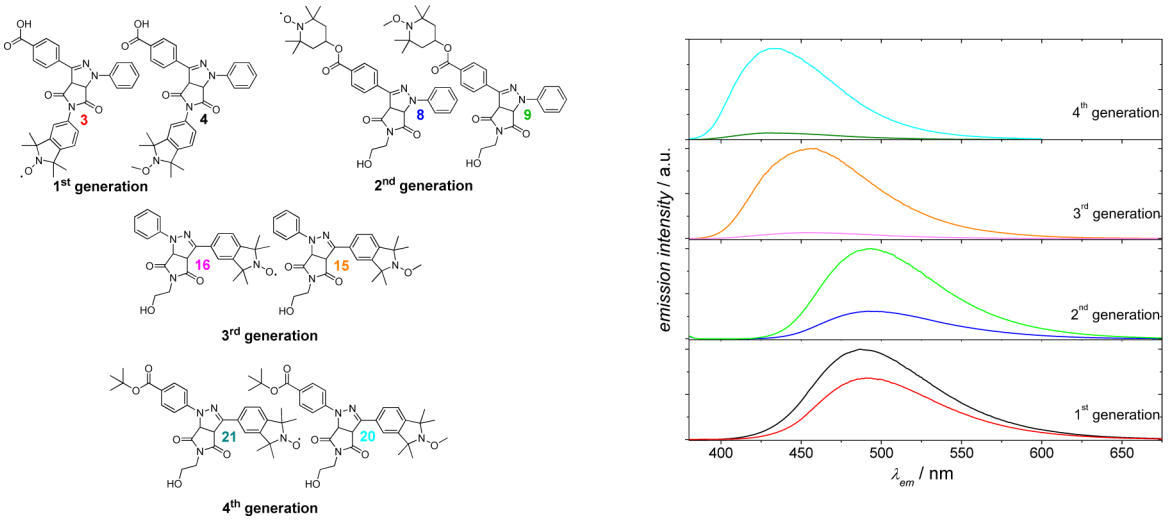

Figure 3. Normalized fluorescence emission spectra of radical pyrazolines **3**, **8**, **16**, and **21** and corresponding methoxyamines **4**, **9**, **15**, and **20** (for assignments of traces see Table 1) in ACN, λ_{ex} = 377 nm (spectra of the radical pyrazoline and the corresponding methoxyamine were optically matched based on their UV absorbance at the excitation wavelength). Spectral lines have been color-coded with the structure numbers above for simple identification.

Scheme 4. Synthesis of Nitroxide Diaryl Tetrazole 14[a]

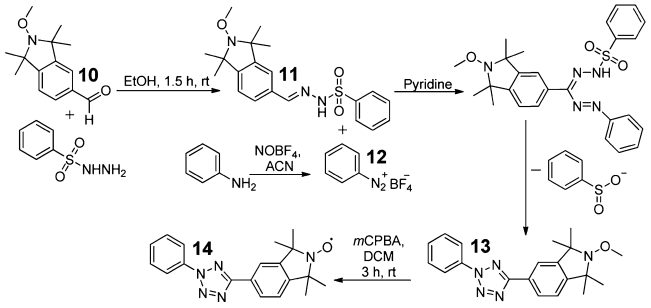

[a]Phenylsulfonylhydrazone **11** was formed from nitroxide **10** and benzenesulfonohydrazide. The arenediazonium salt **12** was formed from aniline. The methoxyamine **13** was oxidized to radical diaryl tetrazole **14** using *m*CPBA.

Scheme 5. NITEC of Radical Diaryl Tetrazole 14 or Methoxyamine 13 and Maleimide 7 To Form the Radical Pyrazoline 16 or Methoxyamine 15, Respectively

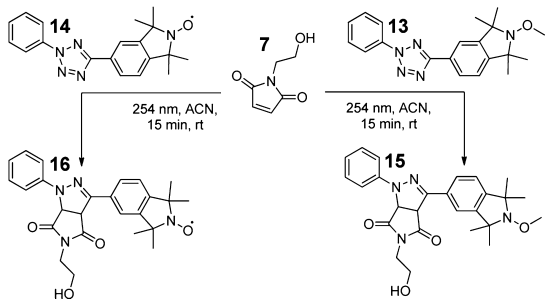

tetrazole species are well-known for fast formation of pyrazolines when activated dipolarophiles such as maleimides or maleic acid derivatives are employed. The ability of the nitroxide functionalized tetrazole **14** to perform in a NITEC reaction with no apparent influence from the nitroxide is surprising. An efficient quenching of excited state of species **14** during irradiation with UV can be assumed, since the distance between the free radical and the tetrazole core is significantly shorter compared to the first- and second-generation products. However, the nitroxide functionalized diaryl tetrazole **14** was still able to undergo the NITEC reaction with high efficiency. It is notable that the presence of the nitroxide species appears to have no significant effect on the NITEC reaction. Identical reactions times, concentrations, solvent, and temperature were applied for formation of both the nonradical pyrazoline **15** and radical-containing pyrazoline **16**. Both reactions lead to full conversion of diaryl tetrazole species and give similar yields for the corresponding pyrazoline.

The fluorescence emission spectra of nonradical pyrazoline **15** and nitroxide-containing pyrazoline **16** are compared in Figure 3. The quenching performance for the third-generation pyrazoline PFNs is improved in comparison to the first- and second-generation species. A much stronger fluorescence quenching effect (ca. 31-fold compared with the diamagnetic species) was observed for adduct **16**. The enhanced quenching performance can be attributed to the extremely short distance between the single electron of the nitroxide and the fluorescent pyrazoline moiety compared to the previous pyrazoline analogues (3.5 Å versus 9.3 and 5.5 Å for **3** and **8**, respectively, see Figure 2), which is of a similar performance to that of currently employed PFNs.[1] Moreover, for the third generation of adducts, the π system of the fluorophore lies in the same plane as the nitroxide 2p orbital, thus allowing maximum overlap (Figure 2).

Fusing the nitroxide directly to the aryl ring of the tetrazole also demonstrates that further functionality can be introduced to these rings. As attachment to biologically relevant molecules or surfaces is a valuable potential application for these probes, attempts to introduce further functionality to compound **15** were undertaken. This was achieved by substituting the diazonium tetrafluoroborate salt **17** to give the *tert*-butyl ester functionalized diaryl tetrazole species **18**. Again, **18** could be deprotected using *m*CPBA to afford the corresponding radical derivative **19** (Scheme 6), and both were able to be exploited for the formation of the functional derivative of the third generation of profluorescent pyrazolines using NITEC chemistry. The *tert*-butyl ester of the diaryl tetrazoles **18** and **19** can be easily converted to a carboxylic acid moiety via

DOI: 10.1021/acs.joc.5b01088
J. Org. Chem. 2015, 80, 8009−8017

Scheme 6. Synthesis of Radical Diaryl Tetrazole 19[a]

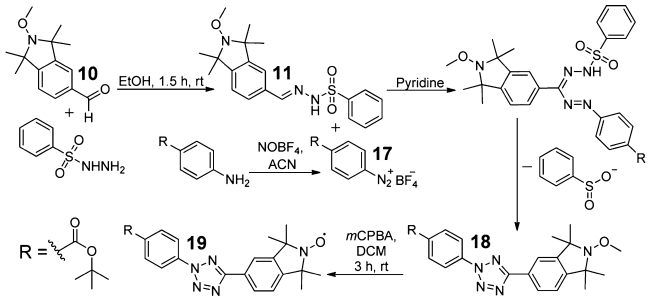

[a]Phenylsulfonylhydrazone **11** was formed from methoxyamine **10** and benzenesulfonohydrazide. Arenediazonium salt **17** was formed from aniline. The methoxyamine **18** was oxidized to radical diaryl tetrazole **19**.

hydrolysis. The resultant carboxylic acid functional group can be employed for further coupling using ester or amide reactions.

Compounds **18** and **19** were converted in the presence of hydroxy functionalized maleimide **7** via NITEC to the corresponding pyrazolines **20** and **21** (Scheme 7). The

Scheme 7. NITEC of Radical Diaryl Tetrazole 19 and Methoxyamine 18 and Maleimide 7 To Form Radical Pyrazoline 21 or Methoxyamine 20, Respectively

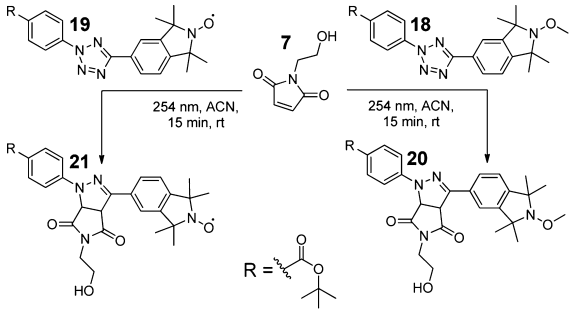

fluorescence emission spectra of the nonradical pyrazoline **20** and nitroxide-containing pyrazoline **21** are compared (Figure 3). Introduction of the ester functionality had little effect on the observed quantum yields with the only photophysical change that could be observed was a slight red-shift of the emission spectra. The quenching performance remained efficient with a ca. 21-fold quenching effect for the radical species **21** compared to the diamagnetic derivative **20** since the calculated distance and orientation between the nitroxide and the fluorophore is similar to the parent third-generation molecule.

The coherence between the distance of the nitroxide species and the fluorophore for all the synthesized cycloadducts is depicted in Figure 3. The corresponding extinction coefficients and quantum yields are listed in Table 1. As noted above, increased proximity between the nitroxide and the fluorophore as well as conjugation between both moieties leads to better quenching performance. The first generation shows the poorest performance as a PFN due to the longer distance between the single electron from the nitroxide moiety and the fluorescent part of the molecule. Furthermore, the five-membered ring in **3** formed during the NITEC reaction decreases the efficiency of coupling between the spin of the single electron and the fluorophore due to nonaromatic nature of the linkage. Comparing the first-generation adducts with the second-

Table 1. Extinction Coefficients and Quantum Yields of Fluorescence for Radical Pyrazolines Derivatives 3, 8, 16, and 21 and Corresponding Methoxyamine Analogues in ACN

cyclo adduct	extinction coefficient ($M^{-1}\cdot cm^{-1}$)	quantum yield (Φ_F)
3	14598	0.369
4	18144	0.436
8	17940	0.18
9	14884	0.58
15	12610	0.50
16	23791	0.016
20	25133	0.77
21	15936	0.036

generation products, the distance between the spin and the fluorophore decreases, giving rise to a better quenching performance for **8**. Moreover, the ester moiety used as a linker can enhance the fluorescence quenching due to increased conjugation within the molecule. For the third generation of nitroxides almost complete fluorescence quenching was observed, since the nitroxide moiety is located in immediate proximity. The quantum yields listed in the Table 1 quantify the visual quenching observation, showing the third pyrazolines to be efficient PFN's with 31- and 21-fold suppression of the quantum yield of fluorescence, respectively. The extinction coefficients vary in the typical range between ca.16000 and 25000 $M^{-1}\cdot cm^{-1}$. Since small amounts of pyrazolines (<1 mg) were used, mass measurement uncertainties could give rise to variations in the extinction coefficients determined. Furthermore, subtle structural influences in the formed cycloadducts could also impact on these values.

In order to investigate the ability of profluorescent pyrazolines to act as radical or redox process sensors, radical pyrazoline **16** was exposed to model redox conditions and to reactive free radicals. For the redox process simulation, sodium ascorbate (NaAsc) and the nitroxides **3**, **8**, and **16** (ratio 20:1) were dissolved in MeOH. The fluorescence of the resulting mixture was monitored every 2 min for a period of 40 min. Evolution of the fluorescence intensities at 373 nm for each measurement with time is shown in Figure 4. NaAsc is a well-known nitroxide reducing agent. In this case the profluorescent nitroxides are reduced to the hydroxylamine, which is diamagnetic and fluorescent. However, the formation of the

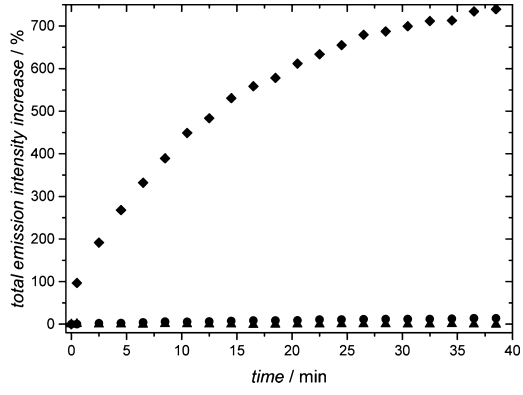

Figure 4. Evolution of the fluorescence emission intensity at 273 nm of the pyrazolines **3** (▲), **8** (●), and **16** (◆) with time in the presence of sodium ascorbate (NaAsc) in methanol ($c_{pyrazoline}$ = 1.68 × 10^{-5} mol·L^{-1}, ratio pyrazoline/NaAsc: 1/20).

DOI: 10.1021/acs.joc.5b01088
J. Org. Chem. 2015, 80, 8009−8017

hydroxylamine is reversible in the presence of oxygen, since oxygen oxidizes the hydroxylamine back to the nitroxide moiety. Since the experiment was carried out under atmospheric conditions, an excess of NaAsc was used to push the redox equilibrium toward hydroxylamine species. Efficient reduction of the radical pyrazoline **16** was observed under these conditions, while only slight increase in fluorescence emission for **8** (ca. 15%) and no increase in fluorescence for pyrazoline **3** was detected. A dramatic increase of the fluorescence peak intensity of the reaction mixture was detected over the first 35 min, consistent with the formation of the fluorescent hydroxylamine After the first 35 min, the fluorescence reached the maximum plateau indicating the establishment of the equilibrium between the hydroxylamine and the nitroxide. The sensitivity of the nitroxide-containing pyrazoline ($c_{\text{pyrazoline}}$ = 17 μ mol·L^{-1}, c_{NaAsc} = 340 μ mol·L^{-1}, $t_{\text{max fluorescence}}$ = 35 min) toward NaAsc is comparable to the previous reported results for aromatic nitroxides ($c_{\text{pyrazoline}}$ = 3 μ mol·L^{-1}, c_{NaAsc} = 5000 μ mol·L^{-1}, $t_{\text{max fluorescence}}$ = 60 min).[12]

To simulate a reactive radical-containing environment, nitroxide **16** was dissolved in ACN in the presence of AIBN (ratio 1:5). The mixture was purged for 30 min with Argon and heated to 60 °C. The fluorescence of the resulting mixture was monitored every 2 min over a period of 70 min. At 60 °C AIBN forms reactive carbon centered radicals. The resultant radicals undergo a rapid recombination reaction with the nitroxide, and a fluorescence intensity increase reflects the sensitivity of the nitroxide functionalized pyrazolines as probes for reactive free radicals. The evolution of the fluorescence peak intensities for each measurement is depicted in Figure 5. After a short

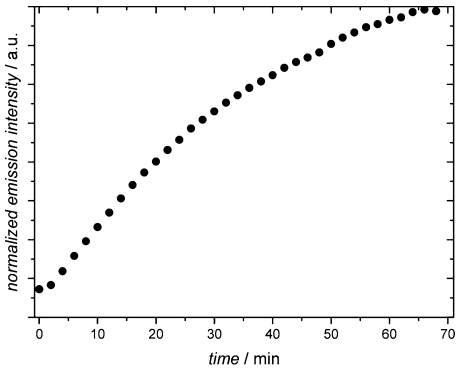

Figure 5. Evolution of the fluorescence emission peak intensity of the radical diaryl tetrazole **16** with time in the presence of AIBN in ACN (c_{16} = 1.68 × 10^{-5} mol·L^{-1}, ratio **16**/AIBN: 1/5). The results for sensitivity of nitroxide-containing pyrazolines toward radicals are in good agreement with the literature.[33] The developed system allows detection of carbon centered radicals at μM concentrations.

induction time, an exponential increase of fluorescence from the reaction mixture was detected over 70 min. A longer time period was needed for reaching the maximum fluorescence intensity in comparison to the reduction experiment using NaAsc. This can be explained by a much smaller excess of AIBN used for the radical termination reaction. Furthermore, incomplete decomposition of AIBN after 70 min and the competing termination reaction between isobutyronitrile radicals will decrease the effective radical concentration in the solution.

CONCLUSIONS

A variety of novel nitroxide functional tetrazol were synthesized and applied along with known tetrazols/maleimide functionalized nitroxides in NITEC reactions in order to introduce a novel, metal-free, photoinduced synthetic path toward profluorescent nitroxides (PFNs) in solution. High reaction rates and full conversion of the components were observed for all synthesized pyrazolines. The presence of the nitroxide species near to the tetrazole did not show any influence on the reaction process. A series of radical pyrazolines and the corresponding methoxyamine analogues formed via NITEC was investigated for their photophysical properties. The fluorescence quenching performance of the cycloadducts is strongly dependent on the distance between the fluorescent part of the molecule and the free radical moiety. The quenching is less efficient if they are further apart, as shown for the first generation and more efficient for the second generation compounds. Almost complete quenching of fluorescence was observed for pyrazolines with direct introduction of nitroxide moiety into the structure of the fluorophore (see third generation). The profluorescent pyrazolines were assessed for their ability to perform as sensors for radical species or redox processes and showed high efficiency in both cases. The introduction of the *tert*-butyl ester in the third generation of pyrazolines allows for further ligation approaches. Our future goal is the translation of the developed sensor technology via the covalent tethering of profluorescent pyrazoline nitroxides to surfaces.

EXPERIMENTAL SECTION

General Methods. Air-sensitive reactions were carried out under an atmosphere of ultrahigh purity argon. 4-(2-phenyl-2H-tetrazol-5-yl)benzoic acid **1** was synthesized according to the literature.[34] All other reagents were purchased from commercial suppliers and used without further purification. ^{1}H and ^{13}C NMR spectra were recorded on a 400 MHz spectrometer and referenced to the relevant solvent peak. ESI high-resolution mass spectra were obtained using a QTOF LC mass spectrometer which utilized ESI (recorded in the positive mode) with a methanol mobile phase. Melting points were measured on a variable-temperature apparatus by the capillary method and are uncorrected. Analytical HPLC was carried out on a HPLC system using a Prep-C18 scalar column (4.6 × 150 mm, 10 μm) with a flow rate of 1 mL/min. All photoreactions were carried out in a Photoreactor with 254 nm lamps (16 x8W).

General Procedure for Time-Resolved Fluorescence Measurments. Reduction with NaAsc: 500 μL stock solution of the desired pyrazoline in MeOH was added to 2.5 mL MeOH, and the fluorescence spectrum was recorded. After adding a stocksolution of NaAsc in MeOH (ca. 30 μL) fluorescence measurements were taken every 2 min for 40 min in total. Radical scavenging: 500 μL stock solution of pyrazoline 16 in acetonitrile was added to 2.5 mL acetonitrile. The solution was purged with argon for 30 min and heated to 60 °C and the fluorescence spectrum was recorded. After adding argon purged stock solution of AIBN in acetonitrile (ca. 30 μL), fluorescence measurements were taken every 2 min for 70 min in total.

Computational Procedures. Geometries of all species were fully optimized using M06L/6-31+G(d), a modern DFT functional chosen for its implicit consideration of dispersion.[35] Calculations were performed in the presence of acetonitrile solvent using the SMD solvent model. All conformations were fully searched at this level of theory to ensure global rather than merely local minima were found, and frequency calculations were performed to confirm the nature of all stationary points. All calculations were performed using the Gaussian 09 software suite.[36]

Synthesis of 5-Maleimido-1,1,3,3-tetramethylisoindolin-2-yloxyl (2). Maleic anhydride (48 mg, 0.49 mmol) was dissolved in

DOI: 10.1021/acs.joc.5b01088
J. Org. Chem. 2015, 80, 8009−8017

2 mL anhydrous Et_2O and added to a solution of 5-amino-1,1,3,3-tetramethylisoindolin-2-yloxyl (100 mg, 0.488 mmol) in 1 mL DCM. The reaction mixture was stirred for 3 h, and the resulting yellow precipitate was recovered by filtration and washed with Et_2O. the isolated solid (116 mg, 0.38 mmol) was then dissolved in 2.5 mL acetic anhydride to which sodium acetate (48 mg, 0.59 mmol) was added. The reaction mixture was stirred for 18 h. After removing the solvent under reduced pressure, the crude product was purified via column chromatography on silica gel using hexane/ethyl acetate (3:2, v/v R_f 0.48) as the eluent. After drying under high vacuum, the title compound **2** was obtained as yellow powder (67 mg, 71%): mp 198 °C; HRMS (EI) *m*/*z*: **2** calcd for $[M + Na]^+$ $C_{16}H_{17}N_2NaO_3$ 308.1137; found 308.1138; EPR (THF) *g* 1.9944, a^N 1.4028.

Synthesis of 1-Oxly-2,2,6,6-tetramethylpiperidin-4-yl 4-(2-phenyl-2H-tetrazol-5-yl)benzoate (6). The hydroxyl functional TEMPO **5** (125.6 mg, 0.73 mmol), DMAP (10.0 mg, 0.08 mmol), and diaryl tetrazole 1 (200 mg, 0.76 mmol) were dissolved in 5 mL THF. After the solution was cooled to 0 °C, DCC (181.6 mg, 0.88 mmol) was added. The reaction mixture was stirred at ambient temperature for 16 h. After THF was removed in vacuum, the obtained solid was dissolved in Et_2O extracted with 1 M hydrochloric acid (2 × 50 mL) and washed with saturated $NaHCO_3$ solution (50 mL). The organic layer was dried over Na_2SO_4, and Et_2O removed under reduced pressure. The crude product was purified via recrystallization in EtOH (2 × 8 mL). The title compound **6** was obtained as pink powder (101 mg, 33%): mp 162−164 °C; HRMS (EI) *m*/*z*: calcd for $[M + Na]^+$ $C_{23}H_{26}N_5NaO_3$ 443.1933; found 443.1925; EPR (THF) *g* 1.9914, a^N 1.5248.

Synthesis of 2-Methoxy-1,1,3,3-tetramethyl-5-(2-phenyl-2H-tetrazol-5-yl)isoindoline (13). A mixture of 2-methoxy-1,1,3,3-tetramethylisoindoline-5-carbaldehyde **10** (114.0 mg, 0.49 mmol) and benzenesulfonohydrazide (84.3 mg 0.49 mmol) in 6.5 mL EtOH was stirred at ambient temperature for 1.5 h. A white precipitate formed after addition of 13 mL water was collected in a funnel. The solid was dissolved in 1.5 mL pyridine (solvent A). In parallel $NOBF_4$ (127.6 mg, 1.09 mmol) was dissolved in 1 mL ACN (dry) under argon. A solution of aniline (100 mg 1.07 mmol) in 3 mL ACN (dry) was added at −30 °C. The reaction mixture was stirred for 20 min at −30 °C and an additional 20 min at room temperature. A white precipitate formed after addition of 15 mL of cold Et_2O (dry) was collected in a funnel. The arenediazonium salt (81 mg, 0.69 mmol) was dissolved in 1 mL ACN and added to solvent A at 0 °C. The reaction mixture was stirred for 3 h at room temperature, diluted in 30 mL ethyl acetate, and extracted with 2 M hydrochloric acid (2 × 100 mL). Ethyl acetate was removed under reduced pressure. The crude product was purified via column chromatography on silica gel using hexane/Et_2O (5:1, v/v R_f 0.51) as the eluent. After drying under high vacuum, the title compound **13** was obtained as yellowish oil (60.0 mg, 35%). ^{1}H NMR (400 MHz, CHLOROFORM-*d*) δ = 8.24−8.12 (m, 3 H), 8.05−7.97 (m, 1 H), 7.61−7.55 (m, 2 H), 7.53−7.47 (m, 1 H), 7.32−7.22 (m, 1 H), 3.81 (s, 3 H), 1.65−1.32 (m, 12 H); ^{13}C NMR (100 MHz, chloroform) δ = 165.3, 147.9, 146.1, 136.9, 129.6, 126.3, 126.2, 122.1, 120.3, 119.8, 67.1, 65.5; HRMS (EI) *m*/*z*: calcd for $[M + H]^+$ $C_{20}H_{24}N_5O$ 350.1981; found 350.1944; HRMS (EI) *m*/*z*: calcd for $[M + H]^+$ $C_{20}H_{24}N_5O$ 350.1981; found 350.1944.

Synthesis of *tert*-Butyl 4-(5-(2-methoxy-1,1,3,3-tetramethylisoindolin-5-yl)-2H-tetrazol-2-yl)benzoate (18). A mixture of 2-methoxy-1,1,3,3-tetramethylisoindoline-5-carbaldehyde **10** (1500.0 mg, 6.44 mmol) and benzenesulfonohydrazide (1120.0 mg 6.44 mmol) in 90 mL EtOH was stirred at ambient temperature for 1.5 h. A white precipitate formed after addition of 180 mL water was collected in a funnel. The solid was dissolved in 20 mL pyridine (solvent A). In parallel $NOBF_4$ (1810.0 mg, 15.47 mmol) was dissolved in 14 mL ACN (dry) under argon. A solution of *tert*-butyl 4-aminobenzoate (2900.0 mg 15.03 mmol) in 10 mL ACN (dry) was added at −30 °C. The reaction mixture was stirred for 10 min at −30 °C and an additional 10 min at room temperature. A white precipitate formed after addition of 50 mL of cold Et_2O (dry) was collected in a funnel. The arenediazonium salt (1530.0 mg, 5.24 mmol) was dissolved in 5 mL ACN and added to solvent A at 0 °C. The reaction mixture was stirred for 3 h at room temperature, diluted in 100 mL ethyl acetate, and extracted with 2 M hydrochloric acid (2 × 400 mL). Ethyl acetate was removed under reduced pressure. The crude product was purified via column chromatography on silica gel using hexane/ethyl acetate (9:1, v/v R_f 0.52) as the eluent. After drying under high vacuum the title compound **18** was obtained as orange oil (630.0 mg, 22%). ^{1}H NMR (400 MHz, chloroform-*d*) δ = 8.30−8.24 (m, 2 H), 8.22−8.12 (m, 3 H), 8.06−7.93 (m, 1 H), 7.27−7.14 (m, 1 H), 3.88−3.76 (m, 3 H), 1.87−1.26 (m, 21 H); ^{13}C NMR (100 MHz, chloroform-*d*) δ = 165.6, 164.5, 148.2, 146.2, 139.4, 132.9, 131.0, 126.4, 125.9, 122.2, 120.4, 119.4, 81.9, 67.2, 65.5, 28.2; HRMS (EI) *m*/*z*: calcd for $[M + H]^+$ $C_{25}H_{32}N_5O_3$ 450.2505; found 450.2483.

Synthesis of 2-Oxyl-1,1,3,3-tetramethyl-5-(2-phenyl-2H-tetrazol-5-yl)isoindoline (14). 2-Methoxy-1,1,3,3-tetramethyl-5-(2-phenyl-2H-tetrazol-5-yl)isoindoline **13** (20 mg, 0.06) was dissolved in 1 mL DCM. *m*CPBA (33.7 mg, 0.15 mmol) was added at 0 °C. Reaction mixture was stirred for 3 h at room temperature. Reaction mixture was diluted with DCM and 2 M NaOH (2 × 50 mL). The organic layer was dried over Na_2SO_4, and DCM removed under reduced pressure. The crude product was purified via column chromatography on silica gel using hexane/ethyl acetate (4:1, v/v R_f 0.59) as the eluent. After drying under high vacuum, the title compound **14** was obtained as orange oil (15.8 mg, 82%). HRMS (EI) *m*/*z*: calcd for $[M + Na]^+$ $C_{19}H_{20}N_5NaO$ 357.1566; found 357.1527; EPR (THF) *g* 1.9924, a^N 1.375.

Synthesis of *tert*-Butyl 4-(5-(2-oxyl-1,1,3,3-tetramethylisoindolin-5-yl)-2H-tetrazol-2-yl)benzoate (19). *tert*-Butyl 4-(5-(2-methoxy-1,1,3,3-tetramethylisoindolin-5-yl)-2H-tetrazol-2-yl)benzoate **18** (380 mg, 0.84 mmol) was dissolved in 5 mL DCM. *m*CPBA (398.1 mg, 2.31 mmol) was added at 0 °C. Reaction mixture was stirred for 3 h at room temperature. Reaction mixture was diluted with DCM and 2 M NaOH (2 × 100 mL). The organic layer was dried over Na_2SO_4, and DCM removed under reduced pressure. The crude product was purified via column chromatography on silica gel using hexane/ethyl acetate (9:1, v/v R_f 0.34) as the eluent. After drying under high vacuum, the title compound **19** was obtained as orange oil (350.2 mg, 96%). HRMS (EI) *m*/*z*: calcd for $[M + Na]^+$ $C_{24}H_{28}N_5NaO_3$ 457.2090; found 457.2080; EPR (THF) *g* 1.9920, a^N 1.4058.

Synthesis of Pyrazoline Derivatives 4-(5-(2-Oxyl-1,1,3,3-tetramethylisoindolin-5-yl)-4,6-dioxo-1-phenyl-1,3a,4,5,6,6a-hexahydropyrrolo[3,4-*c*]pyrazol-3-yl)benzoic acid (3)*, 1-Oxyl-2,2,6,6-tetramethylpiperidin-4-yl 4-(5-(2-hydroxyethyl)-4,6-dioxo-1-phenyl-1,3a,4,5,6,6a-hexahydropyrrolo[3,4-*c*]pyrazol-3-yl)benzoate (8), 5-(2-Hydroxyethyl)-3-(2-methoxy-1,1,3,3-tetramethylisoindolin-5-yl)-1-phenyl-1,6a-dihydropyrrolo[3,4-*c*]pyrazole-4,6(3aH,5H)-dione (15), 5-(2-Hydroxyethyl)-3-(2-oxyl-1,1,3,3-tetramethylisoindolin-5-yl)-1-phenyl-1,6a-dihydropyrrolo[3,4-*c*]pyrazole-4,6(3aH,5H)-dione (16), *tert*-Butyl 4-(5-(2-hydroxyethyl)-3-(2-methoxy-1,1,3,3-tetramethylisoindolin-5-yl)-4,6-dioxo-4,5,6,6a-tetrahydropyrrolo[3,4-*c*]-pyrazol-1(3aH)-yl)benzoate (20), *tert*-Butyl 4-(5-(2-hydroxyethyl)-3-(2-oxyl-1,1,3,3-tetramethylisoindolin-5-yl)-4,6-dioxo-4,5,6,6a-tetrahydropyrrolo[3,4-*c*]pyrazol-1(3aH)-yl)benzoate (21) (see Supporting Information for details). Diaryl tetrazole derivative was dissolved in acetonitrile. Maleimide derivative was added. After irradiation with UV (254 nm) at ambient temperature for 15 min, solvent was removed under reduced pressure. The crude product was purified via column chromatography on silica gel using hexane/ethyl acetate as the eluent. ^{1}H NMR (400 MHz, chloroform-*d*): **15** δ = 7.92 (m, 1 H), 7.85−7.75 (m, 1 H), 7.63−7.51 (m, 2 H), 7.43−7.31 (m, 2 H), 7.22−7.10 (m, 1 H), 7.05−6.95 (m, 1 H), 5.20 (d, *J* = 11.0 Hz, 1 H), 4.93 (d, *J* = 10.9 Hz, 1 H), 3.80 (s, 3 H), 3.84−3.72 (m, 4 H), 2.03−1.91 (m, 1 H), 1.67−1.26 (m, 12 H). **20** δ = 8.02−7.91 (m, 3 H), 7.81−7.72 (m, 1 H), 7.59−7.50 (m, 2 H), 7.21−7.15 (m, 1 H), 5.29 (d, *J* = 10.7 Hz, 1 H), 4.98 (d, *J* = 10.8 Hz, 1 H), 3.79 (s, 3 H), 3.85−3.73 (m, 4 H), 1.59−1.41 (m, 21 H). ^{13}C NMR (100 MHz, chloroform-*d*) **15** δ = 173.3, 172.3, 147.1, 145.8, 144.6, 142.9, 129.4, 129.2, 126.6, 121.7, 121.5, 120.2, 114.4, 67.1, 65.5, 65.5, 60.0, 53.6, 42.3; **20** δ = 172.7, 171.9, 165.8, 147.5, 147.1, 145.9, 144.2, 131.0, 129.0, 126.8, 124.4, 121.8, 120.4, 113.3, 80.5, 67.1, 65.5, 64.5, 59.7, 53.6, 42.3, 28.3. HRMS (EI) *m*/*z*: **3** calcd for $[M + Na]^+$

DOI: 10.1021/acs.joc.5b01088
J. Org. Chem. 2015, 80, 8009−8017

$C_{30}H_{27}N_4NaO_5$ 546.1879; found 546.1867; **8** calcd for $[M+2H]^+$ $C_{29}H_{35}N_4O_6$ 535.2557; found 535.2528; **15** calcd. for $[M + H]^+$ $C_{26}H_{31}N_4O_4$ 463.2345; found 463.2315; **16** calcd for $[M + Na]^+$ $C_{25}H_{27}N_4NaO_4$ 470.1930; found 470.1930; **20** calcd for $[M + H]^+$ $C_{31}H_{39}N_4O_6$ 563.2870; found 563.2828; **21** calcd for $[M + Na]^+$ $C_{30}H_{35}N_4NaO_6$ 570.2454; found 570.2373; EPR (THF) **3** *g* 1.9932, a^N 1.4394; **8** *g* 1.9918, a^N 1.5308; **16** *g* 1.9918, a^N 1.4061; **21** *g* 1.9920, a^N 1.4000.

Synthesis of 4-(5-(2-Methoxy-1,1,3,3-tetramethylisoindolin-5-yl)-4,6-dioxo-1-phenyl-1,3a,4,5,6,6a-hexahydropyrrolo[3,4-*c*]pyrazol-3-yl)benzoic acid (4).** 4-(5-(2-oxyl-1,1,3,3-tetramethylisoindolin-5-yl)-4,6-dioxo-1-phenyl-1,3a,4,5,6,6a-hexahydropyrrolo-[3,4-*c*]pyrazol-3-yl)benzoic acid **3** (20.1 mg, 0.04 mmol) and $FeSO_4 \cdot 7H_2O$ (27.8 mg, 0.1 mmol) were dissolved 0.5 mL DMSO. H_2O_2 (16 μL, 0.14 mmol) was added slowly at 0 °C. Reaction mixture was stirred for 45 min. Thirty mL 2 M HCl was added. The aqueous phase was extracted with Et_2O (4 × 10 mL). The organic layer was dried over Na_2SO_4, and DCM removed under reduced pressure. The crude product was purified via column chromatography on silica gel using hexane/ethyl acetate/acetic acid (2:1:0.01, v/v/v R_f 0.65) as the eluent. After drying under high vacuum, the title compound **4** was obtained as yellow oil (15.2 mg, 73%) ^{1}H NMR (400 MHz, chloroform-*d*): δ = 8.21−8.15 (m, 4 H), 7.68−7.66 (m, 2 H), 7.41−7.37 (m, 2 H), 7.17−7.09 (m, 2 H), 7.04−6.96 (m, 2 H), 5.38 (d, *J* =11.05 Hz, 1 H), 5.7 (d, *J* = 11.06 Hz, 1 H), 1.47−1.35 (m, 12 H); HRMS (EI) *m*/*z*: calcd for $[M + H]^+$ $C_{31}H_{31}N_4O_5$ 539.2294; found 539.2306; ^{13}C NMR (100 MHz, chloroform-*d*) δ = 173.03,172.21, 167.42, 146.03, 145.74, 144.44, 143.40, 135.09, 131.55, 131.21, 129.58, 129.88, 127.38, 126.82, 122.78, 121.53, 120.97, 114.52, 67.10, 66.34, 65.52, 54.24.

Synthesis of 1-Methoxy-2,2,6,6-tetramethylpiperidin-4-yl 4-(5-(2-hydroxyethyl)-4,6-dioxo-1-phenyl-1,3a,4,5,6,6a-hexahydropyrrolo[3,4-*c*]pyrazol-3-yl)benzoate (9). 1-Oxyl-2,2,6,6-tetramethylpiperidin-4-yl 4-(5-(2-hydroxyethyl)-4,6-dioxo-1-phenyl-1,3a,4,5,6,6a-hexahydropyrrolo[3,4-*c*]pyrazol-3-yl)benzoate **8** (7.0 mg, 0.01) and $FeSO_4 \cdot 7H_2O$ (9.3 mg, 0.03 mmol) were dissolved 0.17 mL DMSO. H_2O_2 (8.6 μL, 0.08 mmol) was added slowly at 0 °C. Reaction mixture was stirred for 45 min. 30 mL 2 M HCl was added. The aqueous phase was extracted with Et_2O (4 × 10 mL). The organic layer was dried over Na_2SO_4, and Et_2O removed under reduced pressure. The crude product was purified via column chromatography on silica gel using hexane/ethyl acetate (3:2, v/v R_f 0.28) as the eluent. After drying under high vacuum the title compound **9** was obtained as yellow oil (5.1 mg, 70%). ^{1}H NMR (400 MHz, chloroform-*d*) δ = 8.14−8.02 (m, 4 H), 7.64−7.51 (m, 2 H), 7.43−7.30 (m, 2 H), 7.08−6.97 (m, 1 H), 5.33−5.21 (m, 3 H), 4.94 (d, *J* = 11.1 Hz, 1 H), 3.84−3.72 (m, 5 H), 3.64 (s, 3 H), 2.10−1.64 (m, 5 H), 1.32−1.20 (m, 12 H); ^{13}C NMR (100 MHz, chloroform-*d*) δ = 172.8, 172.0, 165.6, 143.8, 141.4, 134.4, 130.8, 129.7, 129.3, 126.7, 122.0, 114.5, 67.6, 65.5, 60.0, 59.8, 53.3, 44.1, 42.4, 33.0, 20.8; HRMS (EI) *m*/*z*: calcd for $[M + H]^+$ $C_{30}H_{37}N_4O_6$ 549.2713; found 549.2706.

■ ASSOCIATED CONTENT

Supporting Information

Purity and characterization, UV absorption spectra, HPLC traces, EPR spectra, ^{1}H and ^{13}C NMR spectra. The Supporting Information is available free of charge on the ACS Publications website at DOI: 10.1021/acs.joc.5b01088.

■ AUTHOR INFORMATION

Corresponding Authors

*E-mail: j.blinco@qut.edu.au.
*E-mail: christopher.barner-kowollik@kit.edu.

Notes

The authors declare no competing financial interest.

■ ACKNOWLEDGMENTS

We gratefully acknowledge financial support from the ATN-DAAD for facilitating a visit of P.L. to the KIT, the ARC Centre of Excellence for Free Radical Chemistry and Biotechnology (CE 0561607), and the ARC Centre for Electromaterials Science (CE CE140100012). P.L. and K.T. thank the Queensland University of Technology for postgraduate research scholarships. M.L.C. acknowledges generous allocations of supercomputing time on the National Facility of the National Computational Infrastructure. C.B.-K. acknowledges continued funding for this project via the STN program of the Helmholtz association and the Karlsruhe Institute of Technology (KIT).

■ REFERENCES

(1) Blinco, J. P.; Fairfull-Smith, K. E.; Morrow, B. J.; Bottle, S. E. *Aust. J. Chem.* **2011**, *64*, 373.
(2) Green, S. A.; Simpson, D. J.; Zhou, G.; Ho, P. S.; Blough, N. V. *J. Am. Chem. Soc.* **1990**, *112*, 7337.
(3) Ballesteros, O. G.; Maretti, L.; Sastre, R.; Scaiano, J. C. *Macromolecules* **2001**, *34*, 6184.
(4) Toniolo, C.; Crisma, M.; Formaggio, F. *Biopolymers* **1998**, *47*, 153.
(5) Pispisa, B.; Mazzuca, C.; Palleschi, A.; Stella, L.; Venanzi, M.; Wakselman, M.; Mazaleyrat, J.-P.; Rainaldi, M.; Formaggio, F.; Toniolo, C. *Chem. - Eur. J.* **2003**, *9*, 4084.
(6) Simpson, E. M.; Ristovski, Z. D.; Bottle, S. E.; Fairfull-Smith, K. E.; Blinco, J. P. *Polym. Chem.* **2015**, *6*, 2962.
(7) Kálai, T.; Hideg, É.; Vass, I.; Hideg, K. *Free Radical Biol. Med.* **1998**, *24*, 649.
(8) Sowers, M. A.; McCombs, J. R.; Wang, Y.; Paletta, J. T.; Morton, S. W.; Dreaden, E. C.; Boska, M. D.; Ottaviani, M. F.; Hammond, P. T.; Rajca, A.; Johnson, J. A. *Nat. Commun.* **2014**, *5*, 5460.
(9) Yapici, N. B.; Jockusch, S.; Moscatelli, A.; Mandalapu, S. R.; Itagaki, Y.; Bates, D. K.; Wiseman, S.; Gibson, K. M.; Turro, N. J.; Bi, L. *Org. Lett.* **2012**, *14*, 50.
(10) Yang, Y.; Zhao, Q.; Feng, W.; Li, F. *Chem. Rev.* **2013**, *113*, 192.
(11) Maiti, S.; Aydin, Z.; Zhang, Y.; Guo, M. *Dalton Transactions* **2015**, *44*, 8942.
(12) Blough, N. V.; Simpson, D. J. *J. Am. Chem. Soc.* **1988**, *110*, 1915.
(13) Coenjarts, C.; García, O.; Llauger, L.; Palfreyman, J.; Vinette, A. L.; Scaiano, J. C. *J. Am. Chem. Soc.* **2003**, *125*, 620.
(14) Hideg, É.; Kálai, T.; Hideg, K.; Vass, I. *Biochemistry* **1998**, *37*, 11405.
(15) Lozinsky, E.; Martin, V. V.; Berezina, T. A.; Shames, A. I.; Weis, A. L.; Likhtenshtein, G. I. *J. Biochem. Biophys. Methods* **1999**, *38*, 29.
(16) Keddie, D. J.; Johnson, T. E.; Arnold, D. P.; Bottle, S. E. *Org. Biomol. Chem.* **2005**, *3*, 2593.
(17) Blinco, J. P.; McMurtrie, J. C.; Bottle, S. E. *Eur. J. Org. Chem.* **2007**, *2007*, 4638.
(18) Micallef, A. S.; Blinco, J. P.; George, G. A.; Reid, D. A.; Rizzardo, E.; Thang, S. H.; Bottle, S. E. *Polym. Degrad. Stab.* **2005**, *89*, 427.
(19) Blinco, J. P.; Fairfull-Smith, K. E.; Micallef, A. S.; Bottle, S. E. *Polym. Chem.* **2010**, *1*, 1009.
(20) Morrow, B. J.; Keddie, D. J.; Gueven, N.; Lavin, M. F.; Bottle, S. E. *Free Radical Biol. Med.* **2010**, *49*, 67.
(21) Kolb, H. C.; Finn, M. G.; Sharpless, K. B. *Angew. Chem., Int. Ed.* **2001**, *40*, 2004.
(22) Morris, J. C.; McMurtrie, J. C.; Bottle, S. E.; Fairfull-Smith, K. E. *J. Org. Chem.* **2011**, *76*, 4964.
(23) Simpson, E. M.; Ristovski, Z. D.; Bottle, S. E.; Fairfull-Smith, K. E.; Blinco, J. P. *Polym. Chem.* **2015**, *6*, 2962.
(24) Martins, C. D. M. G.; Barcarolli, I. F.; de Menezes, E. J.; Giacomin, M. M.; Wood, C. M.; Bianchini, A. *Aquat. Toxicol.* **2011**, *101*, 88.
(25) Clovis, J. S.; Eckell, A.; Huisgen, R.; Sustmann, R. *Chem. Ber.* **1967**, *100*, 60.

DOI: 10.1021/acs.joc.5b01088
J. Org. Chem. 2015, 80, 8009−8017

(26) de Hoog, H.-P. M.; Nallani, M.; Liedberg, B. *Polym. Chem.* **2012**, *3*, 302.
(27) For example see Dietrich, M.; Delaittre, G.; Blinco, J. P.; Inglis, A. J.; Bruns, M.; Barner-Kowollik, C. *Adv. Funct. Mater.* **2012**, *22*, 304.
(28) Song, W.; Wang, Y.; Qu, J.; Madden, M. M.; Lin, Q. *Angew. Chem., Int. Ed.* **2008**, *47*, 2832.
(29) Rodriguez-Emmenegger, C.; Preuss, C. M.; Yameen, B.; Pop-Georgievski, O.; Bachmann, M.; Mueller, J. O.; Bruns, M.; Goldmann, A. S.; Bastmeyer, M.; Barner-Kowollik, C. *Adv. Mater.* **2013**, *25*, 6123.
(30) Blasco, E.; Piñol, M.; Oriol, L.; Schmidt, B. V. K. J.; Welle, A.; Trouillet, V.; Bruns, M.; Barner-Kowollik, C. *Adv. Funct. Mater.* **2013**, *23*, 4011.
(31) Mueller, J. O.; Guimard, N. K.; Oehlenschlaeger, K. K.; Schmidt, F. G.; Barner-Kowollik, C. *Polym. Chem.* **2014**, *5*, 1447.
(32) Fenton, H. J. H. *J. Chem. Soc., Trans.* **1894**, *65*, 899.
(33) Gerlock, J. L.; Zacmanidis, P. J.; Bauer, D. R.; Simpson, D. J.; Blough, N. V.; Salmeen, I. T. *Free Radical Res.* **1990**, *10*, 119.
(34) Dürr, C. J.; Lederhose, P.; Hlalele, L.; Abt, D.; Kaiser, A.; Brandau, S.; Barner-Kowollik, C. *Macromolecules* **2013**, *46*, 5915.
(35) Zhao, Y.; Truhlar, D. G. *J. Chem. Phys.* **2006**, *125*, 194101.
(36) Frisch, M. J.; Trucks, G. W.; Schlegel, H. B.; Scuseria, G. E.; Robb, M. A.; Cheeseman, J. R.; Scalmani, G.; Barone, V.; Mennucci, B.; Petersson, G. A.; Nakatsuji, H.; Caricato, M.; Li, X.; Hratchian, H. P.; Izmaylov, A. F.; Bloino, J.; Zheng, G.; Sonnenberg, J. L.; Hada, M.; Ehara, M.; Toyota, K.; Fukuda, R.; Hasegawa, J.; Ishida, M.; Nakajima, T.; Honda, Y.; Kitao, O.; Nakai, H.; Vreven, T.; Montgomery, J. A., Jr.; Peralta, J. E.; Ogliaro, F.; Bearpark, M.; Heyd, J. J.; Brothers, E.; Kudin, K. N.; Staroverov, V. N.; Kobayashi, R.; Normand, J.; Raghavachari, K.; Rendell, A.; Burant, J. C.; Iyengar, S. S.; Tomasi, J.; Cossi, M.; Rega, N.; Millam, J. M.; Klene, M.; Knox, J. E.; Cross, J. B.; Bakken, V.; Adamo, C.; Jaramillo, J.; Gomperts, R.; Stratmann, R. E.; Yazyev, O.; Austin, A. J.; Cammi, R.; Pomelli, C.; Ochterski, J. W.; Martin, R. L.; Morokuma, K.; Zakrzewski, V. G.; Voth, G. A.; Salvador, P.; Dannenberg, J. J.; Dapprich, S.; Daniels, A. D.; Farkas, O.; Foresman, J. B.; Ortiz, J. V.; Cioslowski, J.; Fox, D. J. *Gaussian 09*; Gaussian, Inc.: Wallingford, CT, 2009.

DOI: 10.1021/acs.joc.5b01088
J. Org. Chem. 2015, 80, 8009−8017